*Progress In Electromagnetics Research Letters, Vol. 4, 91–98, 2008*

# ANALYSIS OF CO-CHANNEL INTERFERENCE AT WAVEGUIDE JOINTS USING MULTIPLE CAVITY MODELING TECHNIQUE

**D. K. Panda and A. Chakraborty**

Department of Electronics and Electrical Communication Engineering
Indian Institute Of Technology
Kharagpur, West Bengal, 721302, India

**S. R. Choudhury**

Department of Electronics Communication Engineering and
Electronics Instrumentation Engineering
College of Engineering and Management Kolaghat
Mecheda, Midnapur (E), WB, 721171, India

**Abstract**—A method of moment based analysis of the co-channel interference at waveguide joints has been presented using Multi Cavity Modeling Technique (MCMT). The proposed analysis has good agreement with the theoretical; CST microwave studio and HFSS simulated data.

## 1. INTRODUCTION

Low cost, low profile two dimensional scanning phased array antennas have wide application in Low Earth Orbit (LEO), Middle Earth Orbit (MEO) and Geostationary Earth Orbit (GEO) satellite communication. Multi-port Power divider has already found wide applications in phased array techniques. At the input of the two dimensional array mainly longitudinal power dividers are in use. Due to faulty workman-ship there may be a gap at the flange joints which causes the power coupling to the neighbor ports. However the problems of theoretical analysis of this power coupling remains unsolved. Effort has been made to model this interference using a regular structure with adding a uniform gap at the joints.

Present work was performed for theoretical analysis of the co-channel interference at waveguide joints using Multi Cavity Modeling

Technique (MCMT) [1]. The technique involves in replacing all the apertures and discontinuities of the waveguide structures, with equivalent magnetic current densities so that the given structure can be analyzed using only Magnetic Field Integral Equation (MFIE). Since only the magnetic currents present in the apertures are considered the methodology involves only solving simple magnetic integral equation rather than the complex integral equation involving both the electric and magnetic current densities.

## 2. FORMULATION OF THEORY

The diagram of a basic flange with two waveguide sections connected with another one with finite gap is shown in Fig. 1 and its cavity modeling and details of region is shown in Fig. 2 which shows that the structures have 4 waveguide regions and 1 cavity region. For the cavity modeling purposes a uniform gap is assumed and also the boundaries are covered with electric conductors. The interfacing apertures between different regions are replaced by equivalent magnetic current densities. The electric field at the aperture is assumed to be

$$\vec{E} = \hat{u}_x \sum_{p=1}^{M} E_{px} e_{px} + \hat{u}_y \sum_{p=1}^{M} E_{py} e_{py} \tag{1}$$

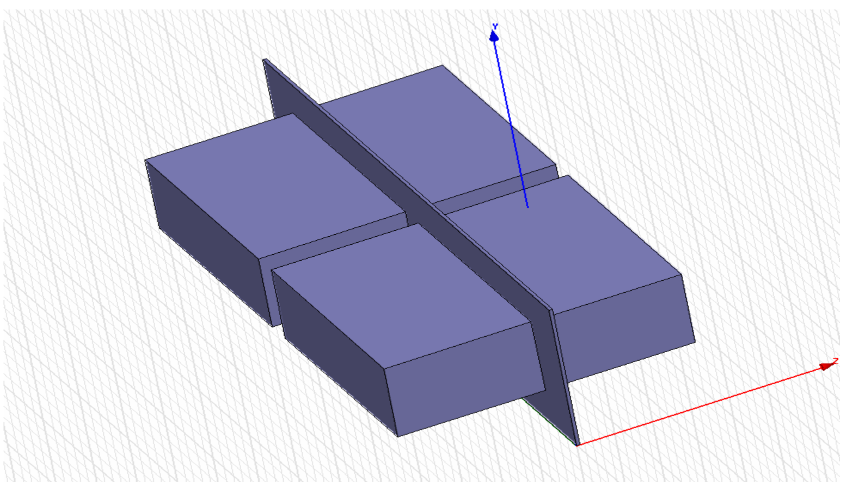

**Figure 1.** Three dimensional view of air passage of two channel waveguide joint.

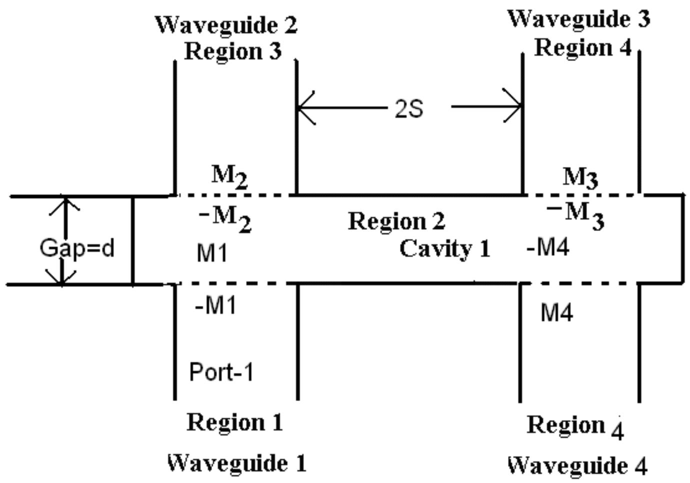


**Figure 2.** Cavity modeling and details of regions of a two channel waveguide joint.

where the basis function $e_p$ $(p = 1, 2, 3 \ldots M)$ are defined by

$$e_p^{i,y} = \begin{cases} \sin\left\{\frac{p\pi}{2L}(x - x_w + L)\right\} & \text{for } \begin{array}{l} x_w - L \le x \le x_w + L \\ y_w - W \le y \le y_w + W \end{array} \\ 0 & \text{elsewhere} \end{cases} \tag{2a}$$

$$e_p^{i,x} = \begin{cases} \sin\left\{\frac{p\pi}{2W}(y - y_w + W)\right\} & \text{for } \begin{array}{l} x_w - L \le x \le x_w + L \\ y_w - W \le y \le y_w + W \end{array} \\ 0 & \text{elsewhere} \end{cases} \tag{2b}$$

In the above expressions:

- $L = a$, $W = b$, $x_w = 0$ and $y_w = 0$ for aperture 1, aperture 2, aperture 3 and aperture 4 with respect to waveguide co-ordinate.
- $L = a$, $W = b$, $x_w = a + s$ and $y_w = 0$ for aperture 1 with respect to cavity axis.
- $L = a$, $W = b$, $x_w = a + s$ and $y_w = 0$ for aperture 2 with respect to cavity axis.
- $L = a$, $W = b$, $x_w = -s - a$ and $y_w = 0$ for aperture 3 with respect to cavity axis.
- $L = a$, $W = b$, $x_w = -s - a$ and $y_w = 0$ for aperture 4 with respect to cavity axis.

where $a = 22.86\,\text{mm}$, $b = 10.16\,\text{mm}$, $S = 1.27\,\text{mm}$ and $2S$ is the distance between waveguide-2 and waveguide-3.

The $X$-component of incident magnetic field at the aperture for the transmitting mode is a dominant $TE_{10}$ mode and is given by

$$H_x^{inc} = -Y_0 \cos\left(\frac{\pi x}{2a}\right) e^{-j\beta z}$$

## 3. EVALUATION OF THE INTERNALLY SCATTERED FIELD

The internally scattered field is obtained by using the modal expansion approach presented in [6]. The internally scattered electric field is given in [3]. Once the electric field is obtained, the corresponding magnetic fields can be derived. The modal voltages are given by (considering only $e_{pq}^{i,tn}$ part of the aperture electric field):

$$V_{mn}^{e} = \sqrt{2ab}\,[E_{px} - E_{py}] \tag{3}$$

$$V_{mn}^{m} = 0 \tag{4}$$

The $x$-component of internally scattered magnetic field can be obtained as,

$$\begin{aligned} H_x^{wvg}\left(E_p^{i,y}\right) &= H_x^{wvg}\left(M_p^{i,x}\right) \\ &= \begin{cases} -\sum\limits_{m=1}^{\infty} Y_{m0}^{e} \sin\left\{\dfrac{m\pi}{2a}(x+a)\right\} & \text{for } p=m \text{ and } n=0 \\ 0 & \text{Otherwise} \end{cases} \end{aligned} \tag{5}$$

$$H_x^{wvg}\left(E_p^{i,x}\right) = -H_x^{wvg}\left(M_p^{i,y}\right) = 0 \tag{6}$$

$$H_y^{wvg}\left(E_p^{i,y}\right) = H_y^{wvg}\left(M_p^{i,x}\right) = 0 \tag{7}$$

$$\begin{aligned} H_y^{wvg}\left(E_p^{i,x}\right) &= -H_y^{wvg}\left(M_p^{i,y}\right) \\ &= \begin{cases} \sum\limits_{n=0}^{\infty} Y_{0n}^{e} \sin\left\{\dfrac{n\pi}{2b}(y+b)\right\} & \text{for } p=n \text{ and } m=0 \\ 0 & \mathit{Otherwise} \end{cases} \end{aligned} \tag{8}$$

## 4. EVALUATION OF THE CAVITY SCATTERED FIELD

The tangential components of the cavity scattered fields are derived in [1]. The final form of the tangential components of the cavity scattered field will be same as given in [3], where $L_{cj}$ is the length and $W_{cj}$ is the height of $j$th the cavity. $L_i$ and $W_i$ are the half length and half width of $i$th aperture.

$$\begin{aligned} & H_x^{cav^j}\left(M_i^x\right) \\ &= -\frac{j\omega\varepsilon}{k^2}\sum_{m=1}^{\infty}\sum_{n=0}^{\infty}\frac{\varepsilon_m\varepsilon_n L_i W_i}{2L_{cj}W_{cj}}\left\{k^2-\left(\frac{m\pi}{2L_c}\right)^2\right\}\sin\left\{\frac{m\pi}{2L_{cj}}\left(x+L_{cj}\right)\right\} \\ &\quad\times\cos\left\{\frac{n\pi}{2W_{cj}}\left(y+W_{cj}\right)\right\}\cos\left\{\frac{n\pi}{2W_{cj}}\left(y_w+W_{cj}\right)\right\}\sin c\left\{\frac{n\pi}{2W_{cj}}W_i\right\}F_x(p) \\ &\quad\times\frac{(-1)}{\Gamma_{mn}\sin\left\{2\Gamma_{mn}t_c\right\}}\begin{cases}\cos\left\{\Gamma_{mn}\left(z-t_c\right)\right\}\cos\left\{\Gamma_{mn}\left(z_0+t_c\right)\right\} & z>z_0 \\ \cos\left\{\Gamma_{mn}\left(z_0-t_c\right)\right\}\cos\left\{\Gamma_{mn}\left(z+t_c\right)\right\} & z<z_0\end{cases} \end{aligned} \tag{9}$$

$$\begin{aligned} & H_x^{cav^j}\left(M_i^y\right) \\ &= \frac{j\omega\varepsilon}{k^2}\sum_{m=1}^{\infty}\sum_{n=0}^{\infty}\frac{\varepsilon_m\varepsilon_n L_i W_i}{2L_{cj}W_{cj}}\frac{m\pi}{2L_{cj}}\frac{n\pi}{2W_{cj}}\sin\left\{\frac{m\pi}{2L_{cj}}\left(x+L_{cj}\right)\right\} \\ &\quad\times\cos\left\{\frac{n\pi}{2W_{cj}}\left(y+W_{cj}\right)\right\}\cos\left\{\frac{m\pi}{2L_{cj}}\left(x_w+L_{cj}\right)\right\}\mathrm{sinc}\left\{\frac{m\pi}{2L_{cj}}L_i\right\}F_y(p) \\ &\quad\times\frac{(-1)}{\Gamma_{mn}\sin\left\{2\Gamma_{mn}t_c\right\}}\begin{cases}\cos\left\{\Gamma_{mn}\left(z-t_c\right)\right\}\cos\left\{\Gamma_{mn}\left(z_0+t_c\right)\right\} & z>z_0 \\ \cos\left\{\Gamma_{mn}\left(z_0-t_c\right)\right\}\cos\left\{\Gamma_{mn}\left(z+t_c\right)\right\} & z<z_0\end{cases} \end{aligned} \tag{10}$$

$$\begin{aligned} & H_y^{cav^j}\left(M_i^x\right) \\ &= \frac{j\omega\varepsilon}{k^2}\sum_{m=1}^{\infty}\sum_{n=0}^{\infty}\frac{\varepsilon_m\varepsilon_n L_i W_i}{2L_{cj}W_{cj}}\frac{m\pi}{2L_{cj}}\frac{n\pi}{2W_{cj}}\cos\left\{\frac{m\pi}{2L_{cj}}\left(x+L_{cj}\right)\right\} \\ &\quad\times\sin\left\{\frac{n\pi}{2W_{cj}}\left(y+W_{cj}\right)\right\}\cos\left\{\frac{n\pi}{2W_{cj}}\left(y_w+W_{cj}\right)\right\}\mathrm{sinc}\left\{\frac{n\pi}{2W_{cj}}W_i\right\}F_x(p) \\ &\quad\times\frac{(-1)}{\Gamma_{mn}\sin\left\{2\Gamma_{mn}t_c\right\}}\begin{cases}\cos\left\{\Gamma_{mn}\left(z-t_c\right)\right\}\cos\left\{\Gamma_{mn}\left(z_0+t_c\right)\right\} & z>z_0 \\ \cos\left\{\Gamma_{mn}\left(z_0-t_c\right)\right\}\cos\left\{\Gamma_{mn}\left(z+t_c\right)\right\} & z<z_0\end{cases} \end{aligned} \tag{11}$$

$$\begin{aligned} & H_y^{cav^j}\left(M_i^y\right) \\ &= -\frac{j\omega\varepsilon}{k^2}\sum_{m=1}^{\infty}\sum_{n=0}^{\infty}\frac{\varepsilon_m\varepsilon_n L_i W_i}{2L_{cj}W_{cj}}\left\{k^2-\left(\frac{n\pi}{2W_{cj}}\right)^2\right\}\cos\left\{\frac{m\pi}{2L_{cj}}\left(x+L_{cj}\right)\right\} \\ &\quad\times\sin\left\{\frac{n\pi}{2W_{cj}}\left(y+W_{cj}\right)\right\}\cos\left\{\frac{m\pi}{2L_{cj}}\left(x_w+L_{cj}\right)\right\}\mathrm{sinc}\left\{\frac{m\pi}{2L_{cj}}L_i\right\}F_y(p) \\ &\quad\times\frac{(-1)}{\Gamma_{mn}\sin\left\{2\Gamma_{mn}t_c\right\}}\begin{cases}\cos\left\{\Gamma_{mn}\left(z-t_c\right)\right\}\cos\left\{\Gamma_{mn}\left(z_0+t_c\right)\right\} & z>z_0 \\ \cos\left\{\Gamma_{mn}\left(z_0-t_c\right)\right\}\cos\left\{\Gamma_{mn}\left(z+t_c\right)\right\} & z<z_0\end{cases} \end{aligned} \tag{12}$$

At the region of the window, the tangential component of the magnetic field in the aperture should be identical and applying the proper boundary conditions at the aperture the electric fields can be evaluated [5].

## 5. SOLVING FOR THE ELECTRIC FIELD

To determine the electric field distribution at the window aperture, it is necessary to determine the basis function coefficients $E_p^{i,x/y}$ at both the apertures. Since the each component of the field is described by M basis functions, 8M unknowns are to be determined from the boundary conditions. The Galerkin's specialization of the method of moments is used to obtain 8M-different equations from the boundary condition to enable determination of $E_p^{i,x/y}$ [6]. The weighting function $w_q^{i,x/y}(x, y, z)$ is selected to be of the same form as the basis function $e_p^{i,x/y}$. The weighting function are defined as follows:

$$w_q^{i,y} = \begin{cases} \sin\left\{\dfrac{q\pi}{2L}(x - x_w + L)\right\} & \text{for } \begin{array}{c} x_w - L \le x \le x_w + L \\ y_w - W \le y \le y_w + W \end{array} \\ 0 & \text{elsewhere} \end{cases} \tag{13a}$$

$$w_q^{i,x} = \begin{cases} \sin\left\{\dfrac{q\pi}{2W}(y - y_w + W)\right\} & \text{for } \begin{array}{c} x_w - L \le x \le x_w + L \\ y_w - W \le y \le y_w + W \end{array} \\ 0 & \text{elsewhere} \end{cases} \tag{13b}$$

## 6. REFLECTION COEFFICIENT AND TRANSMISSION COEFFICIENT

The procedure for derivation of reflection and transmission coefficients is given in [7]. Following the same procedure the expressions for $\Gamma$ and $T$ is given by:

$$\Gamma = \frac{E_y^1 + E_y^2}{E_y^{inc}} = -1 - E_1^{1,y} \tag{14}$$

$$T_{21/31} = \frac{E_y^{transmitted}}{E_y^{inc}} = -E_1^{2/3,y} \tag{15}$$

## 7. NUMERICAL RESULTS AND DISCUSSION

Theoretical data for the magnitude of scattering parameters for an H-plane WR-90 waveguide joints with two channels at X-band has been compared with CST Microwave Studio simulated data and HFSS simulation data in Fig. 3.

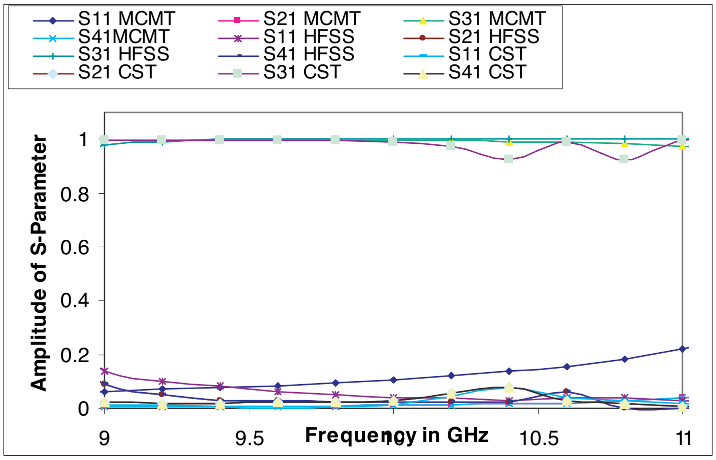


**Figure 3.** Comparison of theoretical, CST Microwave Studio And HFSS simulated data for an H-plane WR-90 waveguide two channel joints with a gap of 0.3 mm.

MATLAB codes have been written for analyzing the structure and numerical data have been obtained after running the codes. The structure was also simulated using CST microwave studio and HFSS. The theory has been validated by the excellent agreement between the theoretical, CST Microwave Studio simulated data and HFSS data. The scattering parameters for the circuit, when excited through port-2, port-3 and port-4 have not been presented in this section because these are also provide same pattern of data as for port-1.

## ACKNOWLEDGMENT

The support provided by Kalpana Chawla Space Technology Cell, IIT Kharagpur is gratefully acknowledged.

## REFERENCES

1. Das, S. and A. Chakraborty, "A novel modeling technique to solve a class of rectangular waveguide based circuits and radiators," *Progress In Electromagnetic Research*, Vol. 61, 231–252, MIT, USA, May 2006.

2. Panda, D. K. and A. Chakraborty, "Multiple cavity modeling of a feed network for two dimensional phased array application," *Progress In Electromagnetics Research Letters*, Vol. 2, 135–140, 2008.
3. Panda, D. K. and A. Chakraborty, "Analysis of a 2:1 rectangular waveguide power combiner using multiple cavity modeling technique," *NCCT-08, Proceedings*, 87–90, India, 2008.
4. Harrington, R. F., *Time-Harmonic Electromagnetic Fields*, McGraw-Hill Book Company, New York, 1961.
5. Collins, R. E., *Field Theory of Guided Waves*, IEEE Press, 1991.
6. Harrington, R. F., *Field Computation by Moment Methods*, Roger E. Krieger Publishing Company, USA, 1982.
7. Das, S., "Analysis of rectangular waveguide based passive devices and antennas using multiple cavity modeling technique," Ph.D. Dissertation, Department of E & ECE, I.I.T Kharagpur, India, 2007.